Journal of Chromatography B, 880 (2012) 148–156

Contents lists available at SciVerse ScienceDirect

Journal of Chromatography B

journal homepage: www.elsevier.com/locate/chromb

Continuous aqueous two-phase extraction of human antibodies using a packed column

P.A.J. Rosa[a], A.M. Azevedo[a], S. Sommerfeld[b], W. Bäcker[b], M.R. Aires-Barros[a,*]

[a] IBB – Institute for Biotechnology and Bioengineering, Centre for Biological and Chemical Engineering, Department of Bioengineering, Instituto Superior Técnico, Technical University of Lisbon, Av. Rovisco Pais, 1049-001 Lisbon, Portugal
[b] Bayer Technology Services GmbH, Building B310, 51368 Leverkusen, Germany

ARTICLE INFO

Article history:
Received 30 June 2011
Accepted 22 November 2011
Available online 30 November 2011

Keywords:
Continuous aqueous two-phase extraction
Packed column
Hold-up
Mass transfer
Human antibodies

ABSTRACT

The performance of a pilot scale packed differential contactor was evaluated for the continuous counter-current aqueous two-phase extraction (ATPE) of human immunoglobulin G (IgG) from a Chinese hamster ovary (CHO) cells supernatant (CS) enriched with pure protein. Preliminary studies have been firstly performed in order to select the dispersed phase (phosphate-rich or polyethylene glycol 3350 Da (PEG)-rich phase) and the column packing material. The PEG-rich phase has been selected as the dispersed phase and the stainless steel as the preferred material for the column packing bed since it was not wetted preferentially by the selected dispersed phase. Hydrodynamic studies have been also performed, and the experimental results were successfully adjusted to the Richardson–Zaki and Mísek equations, typically used for the conventional organic-aqueous two-phase systems. An experimental set-up combining the packed column with a pump mixer-settler stage showed to have the best performance and to be advantageous when compared to the IgG batch extraction. An IgG recovery yield of 85% could be obtained with about 50% of total contaminants and more than 85% of contaminant proteins removal. Mass transfer studies have revealed that the mass transfer was controlled by the PEG-rich phase. A higher efficiency could be obtained when using an extra pump mixer-settler stage and higher flow rates.

1. Introduction

The upstream productivity in the biomanufacturing industry has been progressing remarkably during the last 20 years [1]. These advances are, however, leading to bottlenecks in the downstream processing, since the currently used technological platforms are reaching their limits of throughput and scalability [1]. Liquid–liquid extraction using aqueous two-phase systems (ATPSs) has been suggested as an attractive alternative for the capture of human antibodies from complex cell culture media [2–5]. These systems are spontaneously formed as a result of mutual incompatibility of two polymers or one polymer and salt above certain concentrations in aqueous media. For large-scale processes, polyethylene glycol (PEG)/salt systems have been preferred due to several process advantages including low cost, low viscosity, short phase separation time, wide pH range under which the aqueous two-phase systems are stable and possible recycling strategy of both polymer and salt [6–9]. Besides providing high biocompatibility due to the high water content (70–90% (w/w) water) and the low interfacial tension of these systems [10], high selectivities and recovery yields can be obtained simply by manipulating some experimental conditions, such as phase forming components type and concentration, pH and ionic strength [11]. Moreover, this unit operation can integrate clarification, concentration and purification in just one process step, and combine an easy and reliable scale-up with a continuous mode of operation [10].

The generation of successful bench-scale prototype aqueous two-phase extraction (ATPE) processes with potential commercial application has been reported for the recovery of a large number of biological products [8]. Its technical feasibility has been, however, demonstrated for just few of those biological products. In fact, the poor understanding of the responsible mechanisms for the partitioning of biomolecules in ATPS and the usually used batch equipment assembly (agitated vessel + centrifuge) leads to a certain reluctance from industry to embrace this unit operation as part of their own processes [8]. Column extractors used for the conventional organic–aqueous liquid–liquid extraction (LLE) operations in the chemical industry (e.g. spray and packed column) can be adapted for continuous ATPE of proteins [12] as an alternative to the typically used batch equipment assembly. In fact, they are known to provide more than one theoretical stage improving process efficiency, and do not require the use of a centrifuge to achieve faster phase separation by gravity settling leading to a more cost-effective process [12,13].

* Corresponding author. Tel.: +351 218419065; fax: +351 218419062.
E-mail address: rabarros@ist.utl.pt (M.R. Aires-Barros).

1570-0232/$ – see front matter © 2011 Elsevier B.V. All rights reserved.
doi:10.1016/j.jchromb.2011.11.034

The column extractors are divided into two main categories, namely mechanical agitated (e.g. Scheibel, Karr, rotating-disc and Kuhni contactors) and unagitated and pulsed columns (e.g. spray, packed and sieve tray columns) [14,15]. The agitated contactors may usually be used for liquid–liquid extraction systems characterised by a high interfacial tension, since it is difficult to obtain a good dispersion of these systems in unagitated contactors leading to a poor mass transfer efficiency. Accordingly, the unagitated contactors will be preferred for ATPSs as they are typically characterised by a very low interfacial tension [16]. If agitated contactors would be used for these systems, very small droplets would be formed, probably, leading to emulsification. In addition, the unagitated contactors are characterised by lower investment and operating costs when compared to the agitated contactors [14]. The unagitated spray columns are the simplest and one of the oldest extraction devices. However, despite the very low cost, this type of contactors is rarely used due to the significant axial dispersion (back-mixing) in the continuous phase which, together with a poor phase contact in these extractors, leads to a very low extraction efficiency [14]. The axial mixing in a spray column can be substantially reduced using a sieve tray or a packed column. The packing or the sieve trays will also increase the mass transfer efficiency due to an enhanced interfacial area promoted by the break up of dispersed phase drops [14,15]. Sieve tray columns are, however, more subject to some limitations, such as flooding and entrainment, than packed columns [14]. The packing material selection in a packed column is also an important issue to take into consideration, in order to attain an enhanced mass transfer of the solute. A material preferentially not wetted by the dispersed phase should be preferred in order to avoid the drops coalescence [15]. A further concern is related to the way how the column is packed: regularly or randomly. Regular packings are usually preferred to random packings, as low droplet size dispersions and, consequently, higher mass transfer efficiencies can be obtained. In addition, the higher capacities and lower back-mixing and pressure drops that characterise this type of packing make it advantageous when compared to the conventionally used random packings [15,17].

The technical feasibility of a multi-stage equilibrium ATPE of human antibodies from a Chinese hamster ovary cells (CHO) supernatant has been reported before by Aires-Barros group [18]. A four stages cross-current operation was simulated in a test tube, and an optimised scheme of a predicted counter-current multi-stage ATPE was obtained. Significant improvements, in both recovery yield and purity, were observed when compared to a single-stage extraction step performed at the same experimental conditions. In this report, we have evaluated the performance of a packed extraction column for the continuous counter-current ATPE of human antibodies from a CHO cells supernatant. Several packing materials, including plastic, metal and glass, have been tested in case of phase wetting, and different strategies have been investigated in order to achieve the best contactor performance possible.

2. Experimental

2.1. Chemicals and biologicals

Polyethylene glycol (PEG) with molecular weight of 3350, potassium phosphate dibasic anhydrous (K_2HPO_4), sodium phosphate monobasic anhydrous (NaH_2PO_4) and sodium chloride (NaCl) were obtained from Sigma (St. Louis, MO, USA). All polymers were used without further purification. Human immunoglobulin G (IgG) for therapeutic administration (product name: Gammanorm) was obtained from Octapharma (Lachen, Switzerland), as a 165 mg/mL solution containing 95% of IgG and composed of different percentage of isotypes (59% IgG_1, 36% IgG_2, 4.9% IgG_3 and 0.5% IgG_4). All other chemicals were of analytical grade.

A CHO cells supernatant containing a human immunoglobulin G_1 (IgG_1) directed against a human surface antigen was produced and delivered by Excellgene (Monthey, Switzerland). An Excellgene proprietary serum-free medium containing only one protein was used for production, and phenol red was added to the medium as a pH indicator. According to the enzyme-linked immunosorbent assay (ELISA) determinations performed by Excellgene, the IgG titre was 0.12 mg/mL. Due to the low antibody titre, the supernatant was spiked with 0.5 mg/mL of Gammanorm IgG.

2.2. Aqueous two-phase extraction

2.2.1. Batch extraction

The bottom and top phases of single-stage aqueous two-phase systems were prepared separately by weighting the appropriated amounts of components from stock solutions of 50% (w/w) PEG, 40% (w/w) phosphate buffer and solid NaCl. Phosphate buffer pH 6 was prepared according to the procedure described by Rosa et al. [3]. The pH of the systems was assumed to be the same as the original phosphate stock solution. The bottom phase (BP) was composed of 14.6% (w/w) phosphate pH 6, 0.01% (w/w) PEG 3350, NaCl and 25% (w/w) cells supernatant (CS), and was prepared by mixing a bottom phase stock solution (BPss) with the CS in a mass ratio of 3 to 1, respectively. The top phase (TP) was composed of 29.1% (w/w) PEG 3350, 2.7% (w/w) phosphate pH 6 and NaCl, and was added to the ATPS in two solutions, a 50% (w/w) PEG 3350 (TP1) and a salt solution containing the required phosphate and NaCl (TP2) in the appropriate mass ratio. Partition assays were set up in 15 mL graduated centrifuge tubes. The different solutions (BPss, TP1, TP2 and CS) were weighted into the test tube and mixed in a vortex (Ika, Staufen, Germany). The systems were afterwards incubated at room temperature for about 2 h and centrifuged at 3000 rpm for 10 min for better phase separation (Eppendorf, Hamburg, Germany). Phase volumes were determined and samples from the top and bottom were taken for phase composition analysis. All samples were diluted at least 6 times and analysed against blank phase systems prepared with the same phase composition but adding water instead of the supernatant feed stock.

2.2.2. Continuous extraction

The continuous extraction trials were carried out in a pilot scale glass packed column operating counter-currently. The column had an active mass transfer internal cross section area (A) of 707 mm^2 with an expanded cross section area of 2043 mm^2 in the top. It was composed of nine different sections, in which five of them, with a height of 0.5 m each, contained regular stainless steel (Hastelloy^{TM}) packing (munz type) with an occupancy space of 5–10% of the inner diameter of the column (Sulzer Chemtech GmbH, Linden, Germany). In order to enhance phase separation, the upper part of the column contained a steel mesh as a coalescer. The bottom and top phases were prepared separately as described above for the batch extraction experiments. The column was operated at room temperature in a continuous operation mode, with the top PEG-rich phase being continuously dispersed at the bottom of the column through a capillar and the bottom phosphate-rich phase being continuously fed at the top of the column, as illustrated in Fig. 1.

The continuous phase solutions were first pumped into the column in order to fill the column and wet the packing with that phase, after which the dispersed phase solutions were started to be fed into the column. Both continuous and dispersed phases solutions were mixed in a BKM plastic quadropipe static mixer (Sulzer Chemtech GmbH, Linden, Germany) just before the column inlets.

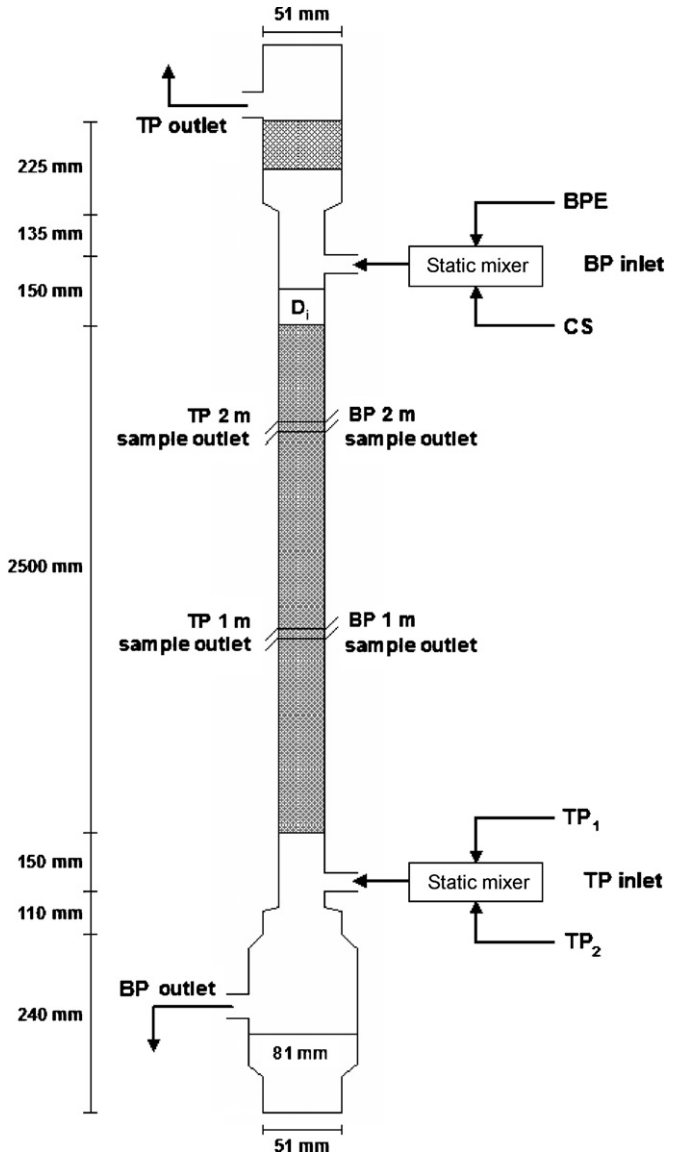

Fig. 1. Experimental set-up of the packed column with an inner diameter (D_i) of 30 mm.

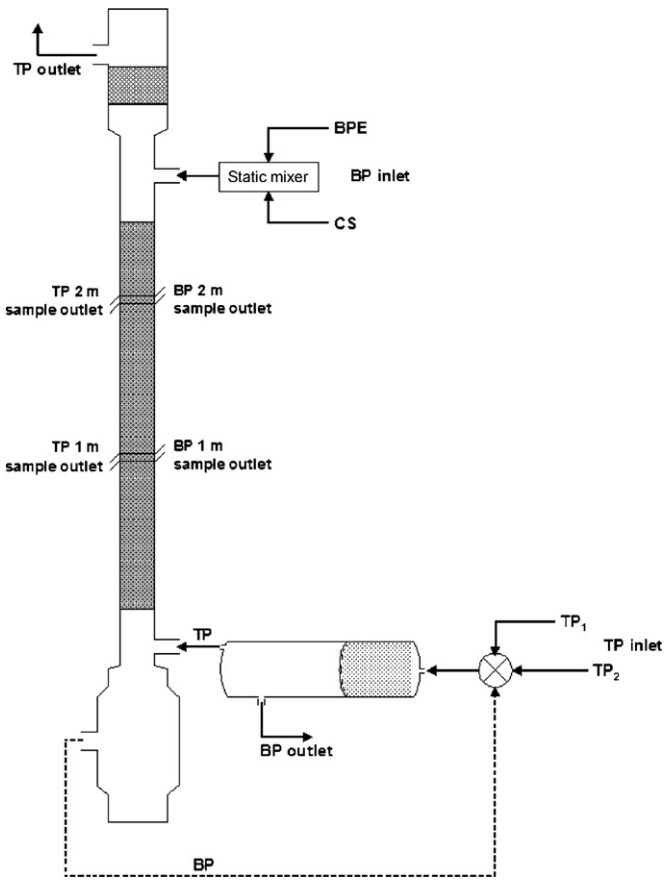

Fig. 2. Experimental set-up of the packed column combined with a pump mixer-settler.

The column was run continuously until steady state was reached. It was considered that the steady state condition was achieved when the liquid hold-up in the column had been replaced at least two to three times and the outlet flow rates and solute concentration were constant after successive measurements. Phase volumes were determined and samples from the PEG-rich and phosphate-rich phases at the bottom and top of the column and at 1 m and 2 m high of the packing bed were taken for composition analysis. A second experimental set-up, where the packed column was combined with a pump mixer-settler, was also tested for the ATPE of IgG (Fig. 2). The pump mixer-settler consisted of a 15 mL pump mixer with a centrally located mixing impeller and a glass settler with 48 mm height and 320 mm length. The dynamic part of the settler contained a metal mesh in order to reduce the volume of the settler.

The hold-up (ϕ) was determined by operating the column until steady flow conditions were reached and stopping simultaneously both inlet and outlet streams. The interface could then be observed to descend slowly due to the accumulation of the dispersed phase. When no further movement of the interface was observed, the continuous phase supply was turned on gradually until all the dispersed phase liquid was collected at the top of the column. The volume of the dispersed phase was then determined, and the hold-up was defined as the volumetric concentration of the dispersed phase in the dispersion.

2.3. Preliminary tests

2.3.1. Dispersed phase selection

Preliminary qualitative tests have been performed in order to select which phase, bottom phosphate-rich or top PEG-rich phase, would be the dispersed phase. A first visual observation test, in which both phases were used as dispersed phases, has been performed in a test tube. With that purpose, two blank ATPSs (without cells supernatant) with the composition described above and volume ratios (V_R), defined as the volume ratio between the top and bottom phase, of 0.4 and 2.5 were prepared. Care was taken that the mixing of both systems was performed equally in order to avoid any interference of this step in the phase settling. The phase separation was observed and the time for complete separation noted. The drop formation was also studied by employing both top PEG-rich and bottom phosphate-rich phases as the dispersed phase. A reservoir was first filled with the supposed continuous phase, and the dispersed phase, previously loaded in a syringe, was slowly injected to allow the formation of individual drops at the needle of the syringe, either at the top or at the bottom of the reservoir, respectively when the phosphate-rich or the PEG-rich phase was the dispersed phase.

2.3.2. Wetting tests

The wet ability of several packing materials for both bottom and top phases was evaluated. A single drop or more of each phase was placed on the upper part of the different packing materials

plates, and its diameter and height was determined. Pictures from the side and top views of the drops were taken with that purpose. The percentage of drop area in the packing material plate (A_{drop}) was calculated according to Eq. (1), where R^2_{drop} corresponds to the radius of the BP or TP drop, respectively, and R^2_{plate} corresponds to the radius of the packing material plate:

$$A_{drop\ \ BP/TP} = \left(\frac{R^2_{drop\ \ BP/TP}}{R^2_{plate}} \right) \times 100. \quad (1)$$

2.4. Analytical methods

2.4.1. Protein A affinity chromatography

The concentration of IgG in both top and bottom phases was determined by protein A affinity chromatography using a Poros protein A affinity column from Applied Biosystems (Foster City, CA, USA) according to the procedure described by Rosa et al. [18]. The recovery yield of IgG in the top phase, Y_{Top}, defined as the ratio between the mass of IgG in the top phase and the total mass of IgG added to the ATPS multiplied by 100, was determined based on the protein A chromatography results. The partition coefficient, K_P, was also determined for the extraction performance evaluation of the batch test tube trials and was defined as the ratio of IgG concentration in the top phase to that in the bottom phase.

2.4.2. Size-exclusion chromatography

The total purity of both top and bottom phases was evaluated by size-exclusion chromatography (SEC) using a TSK-GEL Super SW3000 column (30 cm × 4.6 mm I.D., 4 μm) and a TSK-GEL super SW guard column (3.5 cm × 4.6 mm I.D.) from Tosoh Bioscience (Stuttgart, Germany) according to the procedure described by Rosa et al. [3]. A gel filtration standard containing thyroglobulin, gamma globulin, ovalbumin, myoglobin and vitamin B-12 was used as molecular weight standard. The total purity, P_{Total}, defined as the ratio of the area of the IgG peak to the total area of the chromatogram subtracted by the total area of the blank phase chromatogram, and the percentage of contaminants removal, *CR*, were calculated from the SE chromatograms. The percentage of contaminants removal was obtained according to Eq. (2), where $A_{contaminants}$ is the peak area of the contaminants, *V* is the volume of the corresponding phase and DF is the dilution factor of the sample loaded into the column. The $A_{contaminants}$ was determined by subtracting the area of the IgG peak (A_{IgG}) and the total area of the corresponding blank phase ($A_{total\ blank}$) to the total area of the sample phase chromatogram (A_{total}):

$$CR = \left(1 - \frac{(A_{conta\,\mathrm{min}ants} \times V \times DF)_{Phase}}{(A_{conta\,\mathrm{min}ants} \times V \times DF)_{CHO\ \ cells\ \ supernatant}} \right) \times 100. \quad (2)$$

2.4.3. Total protein quantification

The total protein content in both top and bottom phases was determined by the Bradford assay [19] using a Coomassie reagent supplied by Pierce (Rockford, IL, USA). To avoid interference from phase components, samples were diluted and analysed against blanks containing the same phase composition but without proteins. IgG from Octapharma was used as a standard for protein calibration. The protein purity, $P_{Protein}$, was determined by the ratio of IgG to total protein concentration in the phase, and the purification factor, *PF*, by the ratio between the final purity in the phase and the initial purity in the feed stock.

3. Theory

3.1. Hydrodynamics

The slip velocity concept has been developed to describe the counter- and co-current flow of two heterogeneous phases in a column extractor [20]. This concept concerns the mutual velocities of movement of both liquid phases and states that the average drop rise velocity relative to the continuous phase or slip velocity (v_s) is constant under given conditions, and for counter-current flow is equal to the sum of the average superficial velocities of both dispersed and continuous phase. The superficial velocity of a single phase is defined as the ratio between the volumetric throughput (*F*) and the cross-section area of flow (*A*). In the dispersion, the concept, hence, assumes that the cross-section area accessible for the flow of the dispersed phase is $A\phi$, and for the continuous phase $A(1-\phi)$, according to Eq. (3) [20]:

$$v_s = \frac{v_d}{e\phi} + \frac{v_c}{e(1-\phi)}, \quad (3)$$

where v_d corresponds to the dispersed phase velocity (m/s), v_c corresponds to the continuous phase velocity (m/s) and *e* is a correction factor regarding the space taken by the packing material, corresponding to the void fraction of the packing [21].

The counter-current movement of the dispersed and continuous phases differs significantly from the movement of individual droplets due to either the influence of other droplets or the influence of the ever-present continuous phase. In accordance to that, it has been found that the slip velocity is not constant under certain conditions, being strongly dependent on the hold-up. An increase in the hold-up leads to a decrease in the slip velocity due to the effect called hindered settling [20]. Many studies have been performed in order to better understand this effect, and the following equations have been successfully used for column design of organic–aqueous two-phase systems [20]:

- The Pratt–Thornton equation:

$$v_s = v_0(1-\phi) \quad (4)$$

- The Richardson–Zaki equation:

$$v_s = v_0(1-\phi)^{\alpha} \quad (5)$$

- The Mísek equation:

$$v_s = v_0(1-\phi)\exp(a\phi), \quad (6)$$

where v_0 corresponds to the characteristic rise velocity for a single drop (m/s) and α and ϕ to constants. These three equations describe the departure of slip velocity at $\phi > 0$ from v_0, which is the slip velocity extrapolated to $\phi = 0$ [20].

The limiting operating flow rates are attained when hold-up reaches a maximum value. Any further increase in the dispersed phase flow during the normal operation of column results immediately in flooding, in such a way that, the light phase starts to leave the column at the bottom instead of at the top of the column and the heavy phase the opposite. The hold-up equals to zero when the dispersed phase throughput is zero, increasing, however, when the dispersed phase throughput increases, reaching a maximum attainable which is called as the hold-up at flooding (ϕ_f). Expressing v_d and v_c from Eq. (4) to Eq. (6), differentiating and combining by eliminating v_0, the relations for hold-up at the flooding point are obtained [20]:

- The Pratt–Thornton equation:

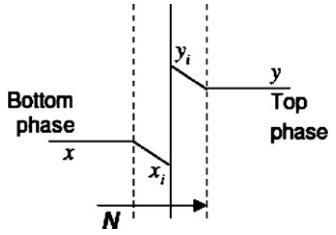

Fig. 3. Concentration gradients across liquid–liquid interface. Adapted from [22].

$$\frac{v_d}{v_c} = \frac{2\phi_f^2}{(1-\phi_f)(1-2\phi_f)} \tag{7}$$

- The Richardson–Zaki equation:

$$\frac{v_d}{v_c} = \frac{(\alpha+1)\phi_f^2}{(1-\phi_f)[1-\phi_f(1+\alpha)]} \tag{8}$$

- The Mísek equation:

$$\frac{v_d}{v_c} = \frac{2\phi_f^2[1-\phi_f+a(\phi_f-\phi_f^2/2-1/2)]}{(1-\phi_f)^2[1-2\phi_f+a(\phi_f-\phi_f^2)]}. \tag{9}$$

3.2. Mass transfer

The mass transfer rate in liquid–liquid extraction processes may be determined by using Whitman's two-film concept, in which the mutual solubility of the two phases is considered negligible, so that the boundary between the two phases will be permeable to the solute. What is more, the interphase mass transfer is assumed to occur by a turbulent mechanism in the main stream of each phase and by a molecular mechanism through stagnant films on each side of the interface, as depicted in Fig. 3 [22]. This process of diffusion occurs because the solute concentration in the bulk of bottom phase is greater than that at the interface, and assuming that the flux across both films is equal, with no resistance at the interface and that the equilibrium is established at the phase boundary [22].

The rate of solute transport across both the films, across the interface, N, may be expressed as:

$$N = k_x(x - x_i) = k_y(y_i - y), \tag{10}$$

where, k_x and k_y are the individual film coefficients for mass transfer (m/s), x and y are the average stream concentrations in both phases (kg/m^3) and x_i and y_i are the solute concentrations in equilibrium across both bottom and top phases at the interface (kg/m^3), with

$$y_i = K_p x_i. \tag{11}$$

The mass transfer rate may be expressed in terms of overall area-based mass transfer coefficients, K_{ox} and K_{oy}, due to the difficulty in determining the interfacial concentrations x_i and y_i [22]:

$$N = K_{ox}(x - x^*) = K_{oy}(y^* - y), \tag{12}$$

where, x^* and y^* represent the solute concentration in the bottom phase in equilibrium with the solute concentration in the bulk of the top phase and the solute concentration in the top phase in equilibrium with the solute concentration in the bulk of the bottom phase, respectively. The overall coefficients, K_{ox} and K_{oy}, can be related to the individual film coefficients through the following equations [22]:

$$\frac{1}{K_{ox}} = \frac{1}{k_x} + \frac{1}{K_p k_y} \tag{13}$$

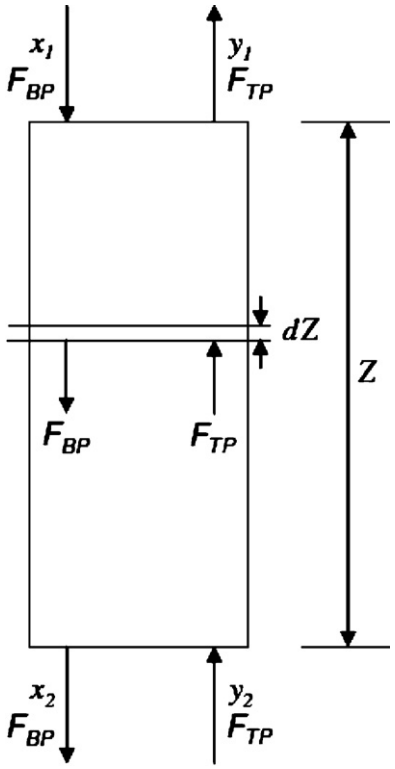

Fig. 4. Scheme of a continuous counter-current differential contactor.

$$\frac{1}{K_{oy}} = \frac{1}{k_y} + \frac{K_P}{k_x}. \tag{14}$$

Fig. 4 shows a schematic diagram for the continuous counter-current extraction of a solute in a differential contactor with a cross sectional area A (m^2). The solute is extracted from the continuous bottom phase, with a flow rate F_{BP} (m^3/s), to the dispersed top phase, with a flow rate F_{TP} (m^3/s).

A differential change in the concentration of both bottom and top phases will occur over a differential height dZ at any location along the column. Thus, if the interfacial area of contact between both phases per volume of active mass transfer volume is a (m^{-1}), then in the differential height dZ, the interfacial area per unit column cross section will be equal to $a(dZ)$ [22]. Accordingly, the rate of solute transfer can be described in terms of overall mass transfer coefficients, $K_{ox}a$ or $K_{oy}a$ (s^{-1}) [22]:

$$d\left(\frac{F_{BP}}{A}x\right) = d\left(\frac{F_{TP}}{A}y\right) = K_{ox}a(x - x^*)dZ = K_{oy}a(y^* - y)dZ. \tag{15}$$

When the solute concentration in the two phases is small, Eq. (15) may be simplified resulting in the following equations [22]:

$$(NTU)_{ox} = \int_{x_2}^{x_1} \frac{dx}{x - x^*} = \frac{A}{F_{BP}} K_{ox}a \int_0^Z dZ = \frac{Z}{(HTU)_{ox}} \tag{16}$$

$$(NTU)_{oy} = \int_{x_2}^{x_1} \frac{dx}{y^* - y} = \frac{A}{F_{BP}} K_{oy}a \int_0^Z dZ = \frac{Z}{(HTU)_{oy}}, \tag{17}$$

where $(NTU)_{ox}$ and $(NTU)_{oy}$ represent the number of transfer units and are a measure of the difficulty of separation, and $(HTU)_{ox}$ and $(HTU)_{oy}$ represent the overall height of transfer unit (m) [22]. Assuming that the equilibrium line is straight with slope K_P and performing a solute mass balance in the whole column, the number of transfer units may be described by the following

equations [22]:

$$(NTU)_{ox} = \int_{x_2}^{x_1} \frac{dx}{x - x^*} = \frac{(x_1 - x_2)}{(x - x^*)_{lm}} = \frac{\ln((x_1 - y_1/K_p)/(x_2 - y_2/K_p))}{1 - (F_{BP}/K_P F_{TP})} \quad (18)$$

$$(NTU)_{oy} = \int_{y_2}^{y_1} \frac{dx}{y^* - y} = \frac{(y_1 - y_2)}{(y^* - y)_{lm}} = \frac{\ln(K_P x_1 - y_1/K_P x_2 - y_2)}{(F_{TP}K_P/F_{BP}) - 1}, \quad (19)$$

where *lm* means log mean of the solute concentration at both top and bottom of the column.

4. Results and discussion

4.1. Preliminary studies

4.1.1. Continuous and dispersed phase selection

The continuous and dispersed phase selection in an LLE process is a relevant issue [23]. In view of that, two different preliminary tests have been performed in order to select which phase, bottom phosphate-rich or top PEG-rich phase, would be the dispersed phase. Two ATPSs with volume ratios of 0.4 (PEG-rich phase used as the dispersed phase) and 2.5 (phosphate-rich phase used as the dispersed phase) were firstly prepared, vigorously mixed and the phases allowed to separate. Photographs were taken at different intervals during phase separation.

It could be clearly observed that, for the lowest volume ratio system, the TP was being dispersed with the droplets rising and coalescing, while, for the highest volume ratio system, the BP droplets were falling and coalescing. A slightly faster phase separation was obtained when the phosphate-rich phase was used as the dispersed phase. However, the obtained droplets were larger and with a non spherical shape when compared to the drops obtained when the PEG-rich phase was dispersed in the phosphate-rich phase. This may be related to the drag force, which results from the higher viscosity of the TP continuous phase when compared to the BP dispersed phase [16]. According to these studies, the PEG-rich phase should be selected as the dispersed phase since, smaller and spherical drops were obtained, which will improve mass transfer efficiency as a consequence of the higher interfacial area.

The drop formation was also evaluated by visual observation by employing both top PEG-rich and bottom phosphate-rich phases as the dispersed phase. Extended films were obtained when the phosphate-rich phase was dispersed in the PEG-rich continuous phase. However, for the opposite case, it was possible to obtain small spherical drops (results not shown). In addition to these experimental visual observations, it is also known from the conventional organic–aqueous liquid–liquid extraction systems that, typically, larger drops are obtained when the solute mass transfer occurs from the dispersed to the continuous phase [22]. These larger drops may result from the solute accumulation in the continuous film between adjacent drops which can lead to an enhanced coalescence due to a local reduction of the interfacial tension [22]. The PEG-rich phase was thus selected as the dispersed phase.

4.1.2. Screening of packing materials: wetting tests

A relevant concern when using a packed extraction column is the packing material wet ability for both continuous and dispersed phases. In fact, the wet ability of the packing surface decides the pattern of flow of the dispersed phase. If the dispersed phase preferentially wets the packing, its flow pattern in the column will be in the form of extended films over the surface of the packing, which may result in a low mass transfer efficiency. In accordance to this, a dispersed phase which does not wet preferentially the packing surface must be preferred, in such a way that, the dispersed phase will flow in the form of discrete drops and the packing will act as baffles and dispersers for the drops [22].

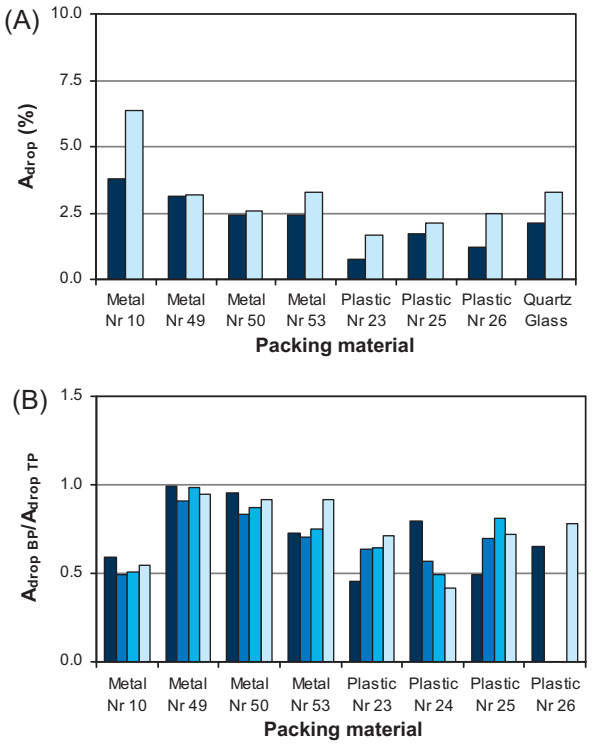

Fig. 5. Wetting tests: (A) percentage of one BP (■) or TP (□) drop area in the several packing material plates evaluated; (B) ratio between BP drop area and TP drop area in the packing material plate: (■) 1 drop, (■) 10 drops, (■) 20 drops and (□) 40 drops. The bottom phase was composed of 14.6% phosphate pH 6, 10.6% NaCl and 0.01% PEG 3350, and the top phase of 29.1% PEG 3350, 8.5% NaCl and 2.7% phosphate pH 6. Concentrations expressed in % (w/w).

The wet ability of several packing materials for both phases was, hence, evaluated as described in the materials and methods section. Fig. 5 depicts the percentage of drop area of both phosphate-rich and PEG-rich phases in the several packing material plates evaluated. A higher percentage of PEG-rich phase drop area and, consequently, a higher PEG-rich phase wetting, was generally observed for the plastic and quartz glass materials in comparison to the phosphate-rich phase. In fact, as shown in Fig. 5B, the ratio $A_{drop\ BP}/A_{drop\ TP}$ was usually higher for the stainless steel materials (except for the Metal Nr 10) indicating that these should be the preferred materials for the column packing bed. The material "Metal Nr 49" was then chosen: it is a regular stainless steel (Hastelloy™) packing (munz type).

4.1.3. Hydrodynamic studies

The influence of the total dispersed and continuous phase velocity on the hold-up was evaluated in order to get some information about the hydrodynamics of the stainless steel packed column running with the selected ATPS according to experimental set-up described in Fig. 1. A regular packing was used due to the advantages already described in the introduction section, such as low droplet size dispersion and, consequently, high mass transfer efficiency, high capacities and low back-mixing and pressure drops. Three different systems with two different NaCl concentrations and using spiked or not spiked cells supernatant have been prepared and the respective hold-up determined (Table 1).

The hold-up describes the amount of solvent actually available for the removal of the target product from the feed, being, hence,

Table 1
Packed column hydrodynamic parameters obtained experimentally and based on the Pratt–Thornton, Richardson–Zaki and Mísek equations using a PEG/phosphate ATPS. The bottom phase was composed of 14.6% phosphate pH 6, NaCl, 0.01% PEG 3350 and 25% CHO cells supernatant, and the top phase of 29.1% PEG 3350, NaCl and 2.7% phosphate pH 6. Concentrations expressed in % (w/w).

Trial	NaCl (%)	CHO CS	$v_c \times 10^3$ (m/s)	$v_d \times 10^3$ (m/s)	ϕ (%)	$v_s \times 10^2$ (m/s)	$\phi_{f\,Pratt-Thornton}$	$\phi_{f\,Richardson-Zaki}$	$\phi_{f\,Misek}$
1	7.5	Without spiking	0.86	0.43	3.6	1.31	–	–	–
2			1.26	0.63	6.5	1.12	–	–	–
3			1.96	0.98	33.4	0.60	28	21	22
4	7.5	Spiked	1.01	0.44	4.0	1.24	27	21	21
5	10	Spiked	1.34	0.80	8.3	1.12	29	22	23

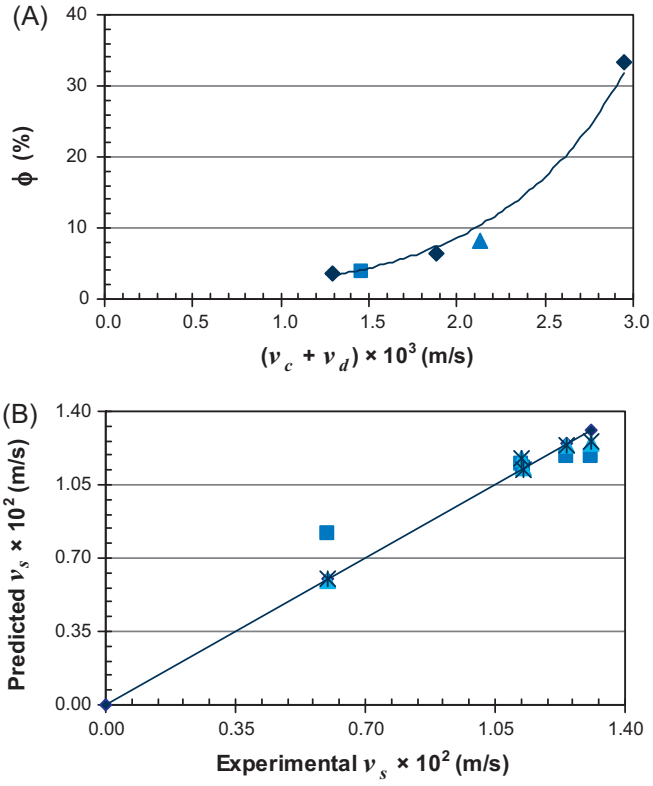

Fig. 6. Hydrodynamic studies: (A) effect of total continuous and dispersed velocity on the hold-up ((♦)) trial 1 to trial 3, (■) trial 4 and (▲) trial 5); (B) parity plot for the slip velocity obtained from Eq. (4) to Eq. (6) ((♦) experimental, (■) Pratt–Thornton, (▲) Richardson–Zaki and (*) Mísek). The bottom phase was composed of 14.6% phosphate pH 6, NaCl and 0.01% PEG 3350, and the top phase of 29.1% PEG 3350, NaCl and 2.7% phosphate pH 6. Concentrations expressed in % (w/w).

valuable for the estimation of the mass transfer capabilities of an extraction unit under defined conditions [24]. An increase in the hold-up was observed as the total continuous and dispersed phase velocities increased (trial 1 to trial 3), being important to notice that the hold-up obtained in trial 3 corresponded to the hold-up at the flooding point. It was also possible to observe that the spiking of the cells supernatant and the increase of the NaCl concentration in the ATPS from 7.5% (w/w) to 10% (w/w) has apparently no significant effect on the hydrodynamics of the column, despite the very low number of experimental points. In fact, these two extra experimental points, corresponding to trial 4 and 5, respectively, fitted well to the hold-up curve obtained for the first three trials (Fig. 6A). The slip velocities were therefore determined, and all the experimental results have been adjusted to the Pratt–Thornton, Richardson–Zaki and Mísek equations [20]:

- The Pratt–Thornton equation:

$$v_s = 1.23 \times 10^{-2}(1-\phi), \quad R^2 = 0.78 \tag{20}$$

- The Richardson–Zaki equation:

$$v_s = 1.34 \times 10^{-2}(1-\phi)^{2.00}, \quad R^2 = 0.99 \tag{21}$$

- The Mísek equation:

$$v_s = 1.36 \times 10^{-2}(1-\phi)\,\exp(-1.24\phi), \quad R^2 = 0.98. \tag{22}$$

Good correlation coefficients were obtained for the adjustments of the experimental data to Richardson–Zaki and Mísek equations (Fig. 6B). For Pratt–Thornton equation, the correlation coefficient was relatively lower. This may be related to the fact that this equation is oversimplified and, indeed, represents only a special case for $\alpha = 1$ or $a = 0$ of the other two equations [20]. As a result, an average characteristic velocity, calculated considering both Eqs. (21) and (22), of 1.35×10^{-2} m/s was attained. This velocity represents, as referred above, the velocity of a single rigid drop and, as expected, is in fact higher than the average drop rise velocity. The limiting hold-up at transition was also determined using Eqs. (7)–(9). The values obtained for the three different trials were very similar, being in average about 21% when the Richardson–Zaki and Mísek equations were used. This value is low when compared to the experimental flooding point obtained, which was 33%. Nevertheless, one should notice that this limiting hold-up at transition occurs at flow rates roughly 50–70% of those resulting in true flooding [21], which means that, actually, the true flooding point hold-up will be close from the one obtained experimentally.

4.2. Aqueous two-phase extraction of IgG using a packed column

4.2.1. Packed column performance

The multi-stage equilibrium ATPE of IgG has been previously investigated by the authors [18]. A four stages cross-current operation was simulated in test tubes for two ATPSs containing 7.5% and 10% (w/w) NaCl. It was observed that, when just 7.5% (w/w) NaCl was added to the ATPS, it was not possible to recover IgG with high yields unless a very high number of stages and/or very high volume ratio would be used [18]. In fact, a volume ratio of 69 and five stages would be required in order to get a 97% IgG recovery yield, leading to a very diluted purified IgG solution [18]. A predicted optimised scheme of a counter-current multi-stage ATPE was, hence, described for the recovery of IgG using a PEG/phosphate ATPS containing 10% (w/w) NaCl. An IgG recovery yield of 89% and protein purity of 75% could be obtained if a volume ratio of 0.4 and five stages would be used, based on McCabe Thiele diagrams [18]. Accordingly, the performance of the regular stainless steel packed column was evaluated for the continuous extraction of IgG from a CHO cells supernatant (570 mg IgG/mL; 700 mg protein impurities/mL, $P_{Protein} = 45\%$, $P_{Total} = 18\%$), using the PEG/phosphate ATPS containing 10% (w/w) NaCl. Trials 1 and 2 were performed under the experimental conditions presented in Table 2 and using different experimental set-ups as depicted in Figs. 1 and 2, respectively. The main difference between both experimental set-ups was the use of an extra pump mixer-settler stage in trial 2. The operating throughputs of both phases were selected to be in the range of 50–80% of the

Table 2
Running conditions of the counter-current ATPE of IgG from a CHO cells supernatant performed in a packed column. The bottom phase was composed of 14.6% phosphate pH 6, 10.6% NaCl, 0.01% PEG 3350 and 25% CHO cells supernatant, and the top phase of 29.1% PEG 3350, 8.5% NaCl and 2.7% phosphate pH 6. Concentrations expressed in % (w/w).

Trials	$F_{BP\,in}$ (L/h)	$F_{CS\,in}$ (L/h)	$F_{TP1\,in}$ (L/h)	$F_{TP2\,in}$ (L/h)	$F_{BP\,out}$ (L/h)	$F_{TP\,out}$ (L/h)	V_R
Test-tube	–	–	–	–	–	–	0.54
Trial 1	1.68	0.73	0.76	0.49	2.25	1.23	0.55
Trial 2	2.57	1.05	1.12	0.77	3.45	2.01	0.58

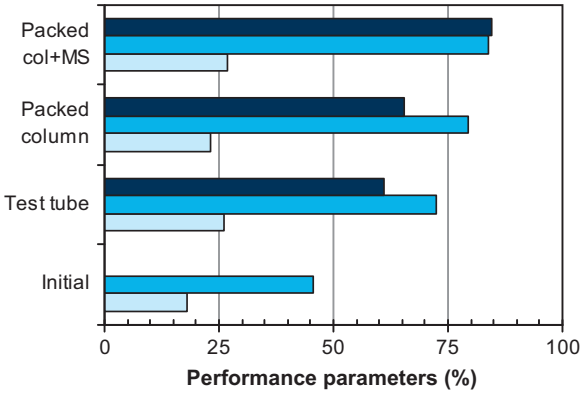

Fig. 7. Performance parameters obtained for the IgG ATPE from a CHO cells supernatant containing 0.57 mg/mL IgG in a test tube, in a counter-current packed column as described in Fig. 1 and in a counter-current packed column combined with a pump mixer-settler (packed column + MS) as described in Fig. 2: (■) Y_{Top}, (■) $P_{Protein}$ and (■) P_{Total}. The bottom phase was composed of 14.6% phosphate pH 6, 10.6% NaCl, 0.01% PEG 3350 and 25% CHO cells supernatant, and the top phase of 29.1% PEG 3350, 8.5% NaCl and 2.7% phosphate pH 6. Concentrations expressed in % (w/w).

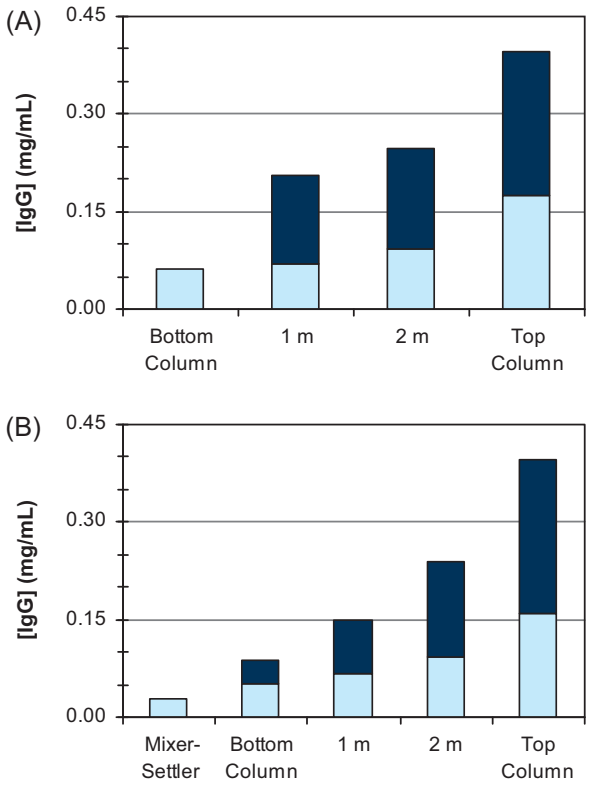

Fig. 8. IgG profile along the column during the ATPE from a CHO cells supernatant using the experimental set-up described in (A) Fig. 1 and (B) Fig. 3: (■) bottom phase and (■) top phase.

limiting value, which is reached at flooding conditions [20]. A batch test tube trial was also performed for comparison. The steady state was reached about 5 h after the beginning of trial 1 and 4 h after the beginning of trial 2.

Fig. 7 shows the extraction performance parameters obtained for the three trials. When the experimental set-up described in Fig. 1 was used, the IgG recovery yield in the PEG-rich phase was similar to the test tube trial. Higher IgG recovery yields were, however, attained when the experimental set-up described in Fig. 2 was used. A 24% higher recovery yield and slightly higher purities were obtained when compared to the batch test tube trial, indicating that the differential contactor combined with a pump mixer-settler allows the continuous recovery of IgG with a higher enrichment without loosing in purity. Moreover, this experimental set-up column + pump mixer-settler allowed the removal of about 50% of total contaminants and more than 85% of contaminant proteins. Similar extraction performance results were previously obtained when the IgG ATPE was performed in a six stages counter-current MSB [18]. It is, hence, possible to conclude that the used experimental set-up differential packed contactor + pump mixer-settler is suitable for the continuous extraction of IgG from a CHO cells supernatant. The IgG profile along the column was also determined for both trial 1 and trial 2, and is depicted in Fig. 8. It can be observed that, as expected according to the extraction performance results, in trial 1, more IgG remains in the phosphate-rich phase.

In order to understand the differences between the results obtained in trials 1 and 2, the recovery yields obtained in trial 2 in the column and in the pump mixer-settler stage were determined. A 73% and 12% recovery yields were obtained in the column and pump-mixer-settler steps, respectively. One may, hence, conclude that the higher yield obtained, using the experimental set-up described in Fig. 2, may not only be related to the fact of having one stage more, but maybe also to the higher flow rates used. In fact, when higher flow rates are used, the average drop rise velocity is lower leading to a higher residence time inside the column and, consequently, an enhanced mass transfer. On the other hand, the mixing of the TP1 and TP2 solutions before the TP inlet in the column in trial 1 could have also been a bottleneck in achieving a high recovery yield. The high viscosity of TP1 might have led to a deficient mixing of the TP solutions, resulting in a heterogeneous dispersed top phase, and, probably, in a lower solute mass transfer from the continuous phosphate-rich phase to the dispersed PEG-rich phase. The fact of having a pump mixer-settler stage before the column in trial 2 assures an efficient mixing of the TP inlet solutions, so that the phases components (especially top phase) will reach equilibrium concentrations before the column inlet. This will translate into higher mass transfer efficiencies in the bottom of the column as the use of a previous stage makes sure that the phase components equilibrium concentrations are reached before the column inlet. A column with a higher active mass transfer height and higher flow rates should then be used in order to enrich higher recovery yields, being, however, necessary to find a commitment between the equipment specifications and hydrodynamics.

4.2.2. Mass transfer studies

The IgG liquid–liquid equilibrium data has been previously determined for the PEG/phosphate ATPS and a dependency of the partitioning coefficient on the IgG concentration was observed,

Table 3
Packed column efficiency parameters obtained for the continuous counter-current ATPE of IgG from a CHO cells supernatant. The bottom phase was composed of 14.6% phosphate pH 6, 10.6% NaCl, 0.01% PEG 3350 and 25% CHO cells supernatant, and the top phase of 29.1% PEG 3350, 8.5% NaCl and 2.7% phosphate pH 6. Concentrations expressed in % (w/w).

Trials	$K_{oy}a \times 10^5$ (s^{-1})	$K_{ox}a \times 10^5$ (s^{-1})	$(NTU)_{oy}$	$(HTU)_{oy}$ (m)
Trial 1	12.2	41.5	0.71	4.0
Trial 2	25.6	87.0	0.91	3.1

especially at very low concentrations [24]. Thus, the IgG partitioning coefficient along the differential contactor was also not constant due to the IgG concentration variation inside the column. In fact, according to LLE data obtained in batch test tube trials [25], it was expected that the IgG partitioning coefficient in the bottom of the column would be low, close from about 1, increasing up to about 6 in the top of the column. As a result, in order to determine the efficiency of the column in both trials 1 and 2 by applying the two-film concept, which assumes a constant partitioning coefficient, an average partitioning coefficient was considered and the continuous and dispersed based overall mass transfer coefficients determined. The average IgG partitioning coefficient was determined based on a linear regression of the LLE data and was found to be 3.4. Table 3 presents the packed column efficiency parameters obtained for the continuous counter-current ATPE of IgG from the CHO cells supernatant. Higher overall mass transfer coefficients were obtained for trial 2, which may be related to the use of higher flow rates and an extra pump mixer-settler stage which allowed the attainment of the phases components equilibrium concentrations before the column inlet. In addition, it is possible to observe that, as expected according to the two-film theory, the mass transfer was controlled by the PEG-rich dispersed phase and, therefore, the calculation of the height and number of transfer units was based on that phase. A slightly higher efficiency of the packed column was observed for trial 2. Further mass transfer and hydrodynamic studies should, however, be performed in order to improve the efficiency of this packed differential contactor for the ATPE of IgG from complex cell culture media.

5. Conclusions

In this research work, the suitability of a packed differential contactor for the ATPE of human antibodies from a CHO cells supernatant is shown. Preliminary studies, based on visual observation and wetting evaluation, revealed that the PEG-rich phase should be used as the dispersed phase and that a stainless steel packing bed should be selected. The hydrodynamics of the stainless steel packed column was further studied, and it was possible to successfully adjust the experimental data to the Pratt–Thornton, Richardson–Zaki and Mísek equations, which have been typically used for the conventional organic–aqueous two-phase systems.

The best performing experimental set-up for the ATPE of IgG consisted of a combination of the packed column with a pump mixer-settler. An IgG recovery yield of 85% and a protein purity of 84% (purification factor of 1.84 out of a maximum of 2.19) were obtained. This represents significant improvements when compared to the batch IgG extraction, where a recovery yield of 61% and purification factor of 1.59 were attained. According to the mass transfer studies, it was also possible to conclude that the use of higher flow rates and an extra pump mixer-settler stage favour the IgG mass transfer, which was controlled by the PEG-rich dispersed phase. A commitment between the equipment specifications and hydrodynamics should, however, be obtained in order to have the higher mass transfer efficiency possible.

Acknowledgements

This work was carried out within the European project AIMs (contract no. NMP3-CT-2004-500160), supported by funding under the Sixth Research Framework Programme of the European Union. P.A.J.R. acknowledges *Fundação para a Ciência e Tecnologia* for a PhD fellowship (BD 25040/2005), and A.M.A. for funding from the programme "Ciência 2007" of the Portuguese Ministry for Science, Technology and Higher Education (http://www.mctes.pt).

References

[1] U. Gottschalk, Biotechnol. Prog. 24 (2008) 496.
[2] B.A. Andrews, S. Nielsen, J.A. Asenjo, Bioseparation 6 (1996) 303.
[3] P.A.J. Rosa, A.M. Azevedo, M.R. Aires-Barros, J. Chromatogr. A 1141 (2007) 50.
[4] P.A.J. Rosa, I.F. Ferreira, A.M. Azevedo, M.R. Aires-Barros, J. Chromatogr. A 1217 (2010) 2296.
[5] A.M. Azevedo, P.A.J. Rosa, I.F. Ferreira, M.R. Aires-Barros, Trends Biotechnol. 27 (2009) 240.
[6] M.J.L. Costa, M.T. Cunha, J.M.S. Cabral, M.R. Aires-Barros, Bioseparation 9 (2000) 231.
[7] A. Greve, M.-R. Kula, J. Chem. Technol. Biotechnol. 50 (1991) 27.
[8] M. Rito-Palomares, J. Chromatogr. B 807 (2004) 3.
[9] M. Rito-Palomares, A. Lyddiatt, J. Chromatogr. B 680 (1996) 81.
[10] P.-Å. Albertsson, Partition of Cell Particles and Macromolecules, Wiley, New York, 1986.
[11] K. Schügerl, J. Hubbuch, Curr. Opin. Microbiol. 8 (2005) 294.
[12] L. Igarashi, T.G. Kieckbush, T.T. Franco, J. Chromatogr. B 807 (2004) 75.
[13] N.D. Srinivas, A.V. Narayan, K.S.M.S. Raghavarao, Process Biochem. 38 (2002) 387.
[14] J.D. Seader, E.J. Henley, Separation Process Principles, John Wiley & Sons, New York, 1998.
[15] A.B. de Haan, H. Bosch, Fundamentals of Industrial Separations, De Haan & Bosch, Eindhoven, 2007.
[16] R.S. Barhate, G. Patil, N.D. Srinivas, K.S.M.S. Raghavarao, J. Chromatogr. A 1023 (2004) 197.
[17] S.Y. Cho, Y.Y. Lee, S.J. Kim, Korean J. Chem. Eng. 12 (1995) 313.
[18] P.A.J. Rosa, A.M. Azevedo, S. Sommerfeld, M. Mutter, M.R. Aires-Barros, W. Bäcker, J. Biotechnol. 139 (2009) 306.
[19] M.M. Bradford, Anal. Biochem. 72 (1976) 248.
[20] T. Mísek, in: J.C. Godfrey, M.J. Slater (Eds.), Liquid–Liquid Extraction Equipment, John Wiley & Sons, West Sussex, 1994, p. 95.
[21] R.E. Treybal, Mass-Transfer Operations, 3rd ed., McGraw-Hill Book Co., Singapore, 1981.
[22] G.S. Laddha, T.E. Degaleesan, Transport Phenomena in Liquid Extraction, Tata McGraw-Hill, New Delhi, 1976.
[23] J.A. Asenjo, S.L. Mistry, B.A. Andrews, J.C. Merchuk, Biotechnol. Bioeng. 79 (2002) 217.
[24] L.A. Sarubbo, L.A. Oliveira, A.L.F. Porto, J.L. Lima-Filho, G.M. Campos-takaki, E.B. Tambourgi, Biochem. Eng. J. 16 (2003) 221.